Reliable metal alloy contact for a $Mg_{3+\delta}Bi_{1.5}Sb_{0.5}$ thermoelectric device

Shaowei Song[a], Zhongxin Liang[a], Congcong Xu[a], Yu Wang[a, b], Xin Shi[a], Wuyang Ren[a, c], Zhifeng Ren[a, *]

[a]Department of Physics and Texas Center for Superconductivity at University of Houston (TcSUH), University of Houston, Houston, Texas 77204, USA
[b]Materials Science and Engineering Program, University of Houston, Houston, Texas 77204, USA
[c]Institute of Fundamental and Frontier Sciences, University of Electronic Science and Technology of China, Chengdu, Sichuan 610054, China

*Author to whom correspondence should be addressed: zren@uh.edu

Table S1. Typical work functions of various metals, metal alloys, and TE materials.

	Work Function (eV)		Work Function (eV)
Ni	5.15	Sb	4.55~5.7
Fe	4.7	Bi	4.31
Al	4.3	Mg	3.66
Cr	4.5	Bi_2Te_3	5.4
Stainless steel	4.3~4.4	$Bi_{0.5}Sb_{1.5}Te_3$	4.5
NiFe (80:20 wt%)	4.8	PbTe	3.9
n-type $Mg_3Sb_{2-x}Bi_x$	3.85		

Table S2. Compositions of contact materials used in this study.

	wt %
NiFe	Ni/Fe = 80:20
Stainless steel	Fe/Cr/Ni/Mo = 67.5:17.0:13.0:2.5
NiCrFe	Ni/Cr/Fe = 72:14~18:12~16
NiCr	Ni/Cr = 80:20
Fe	>99%
Ni	>99%

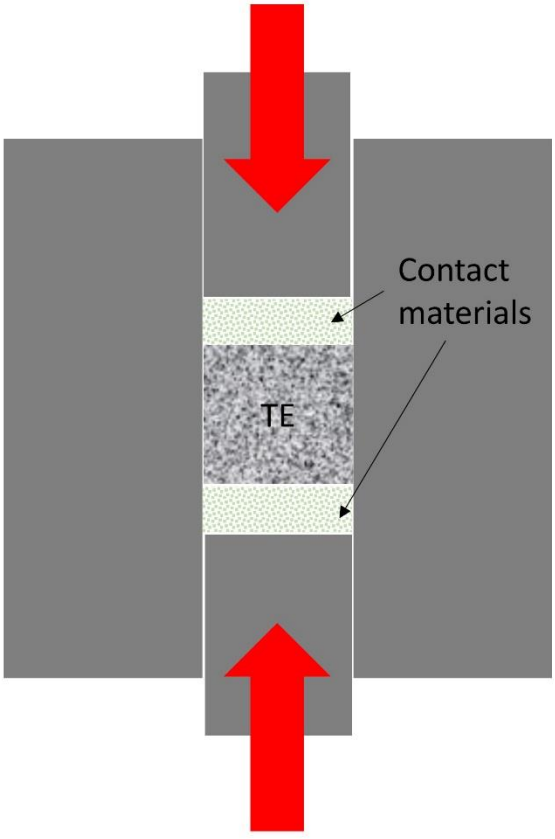

Figure S1. Schematic illustration of one-step hot-pressing to form a contact between a TE material and a metal or metal alloy.

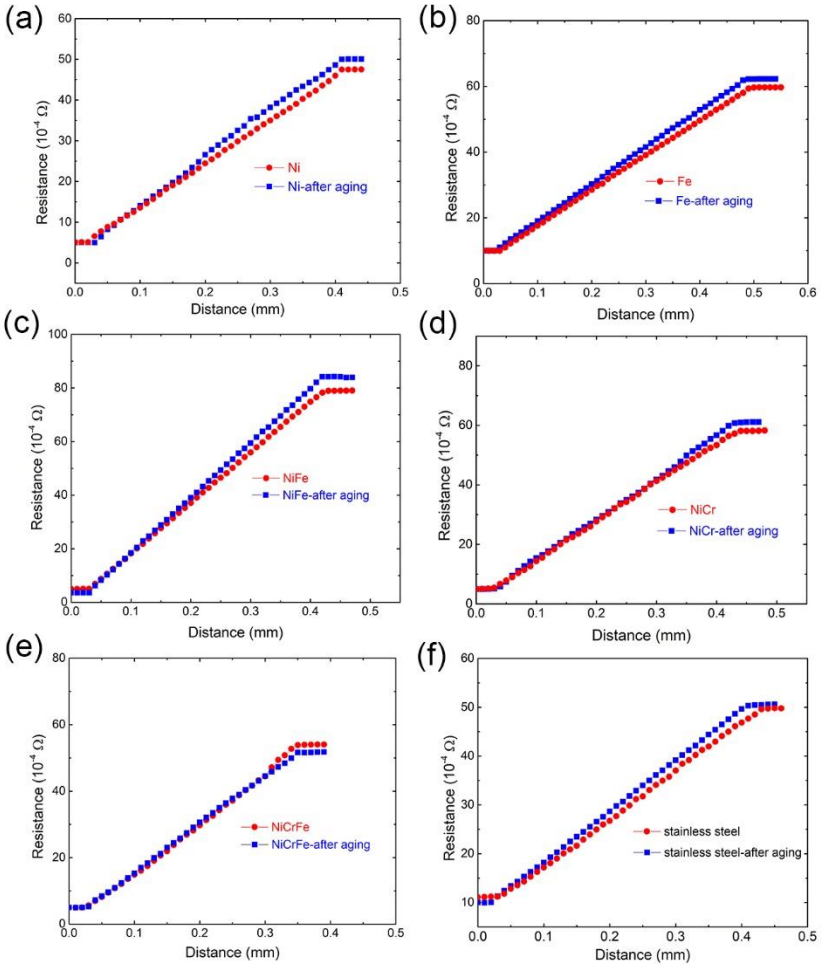

Figure S2. Comparison of measured contact resistivity curves before and after aging for ~2,100 h at 573 K for each as-prepared single TE leg sample.

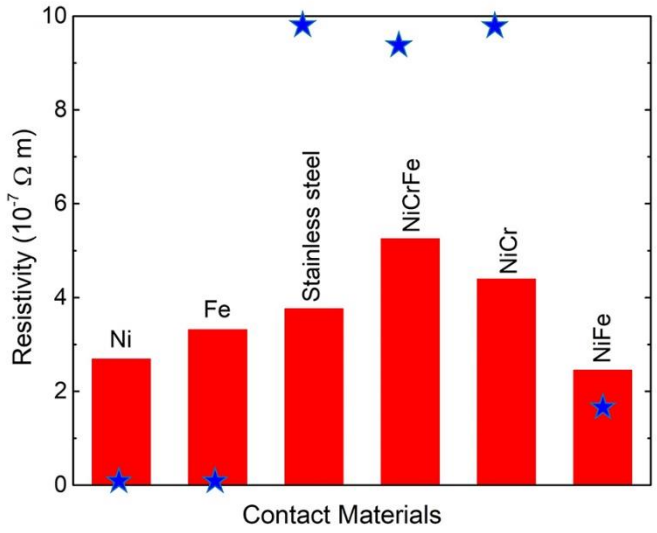

Figure S3. Resistivity of the metals and metal alloys used as contact materials in the single M/TE leg. The data with red pillars were extracted from their slopes in the measurement curve (**Figure** S2), and the data shown as blue stars were obtained through measurements on the commercial ULVAC ZEM-3 after hot-pressing following the procedure for preparing the single M/TE leg.

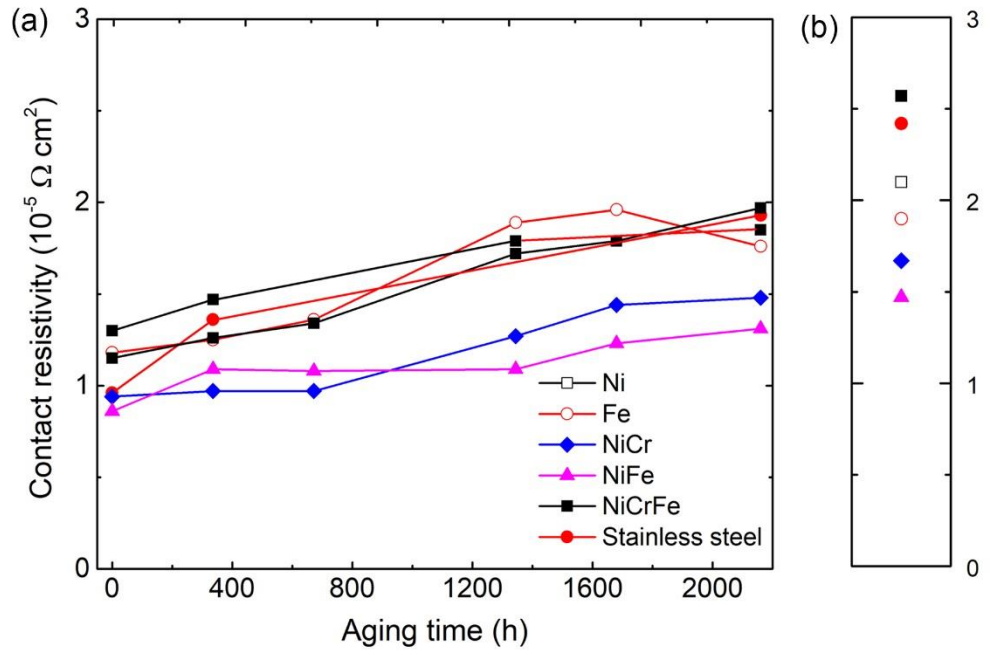

Figure S4. (a) Aging-time dependence of contact resistivity of single M/TE leg composed of n-type $Mg_{3+\delta}Bi_{1.5}Sb_{0.5}$ and different contact materials as specified. (b) Contact resistivity of single M/TE leg composed of n-type $Mg_{3+}Bi_{1.5}Sb_{0.5}$ and different contact materials as specified after thermal failure testing. For clearer readability, error of 1.5%~2% is not shown.

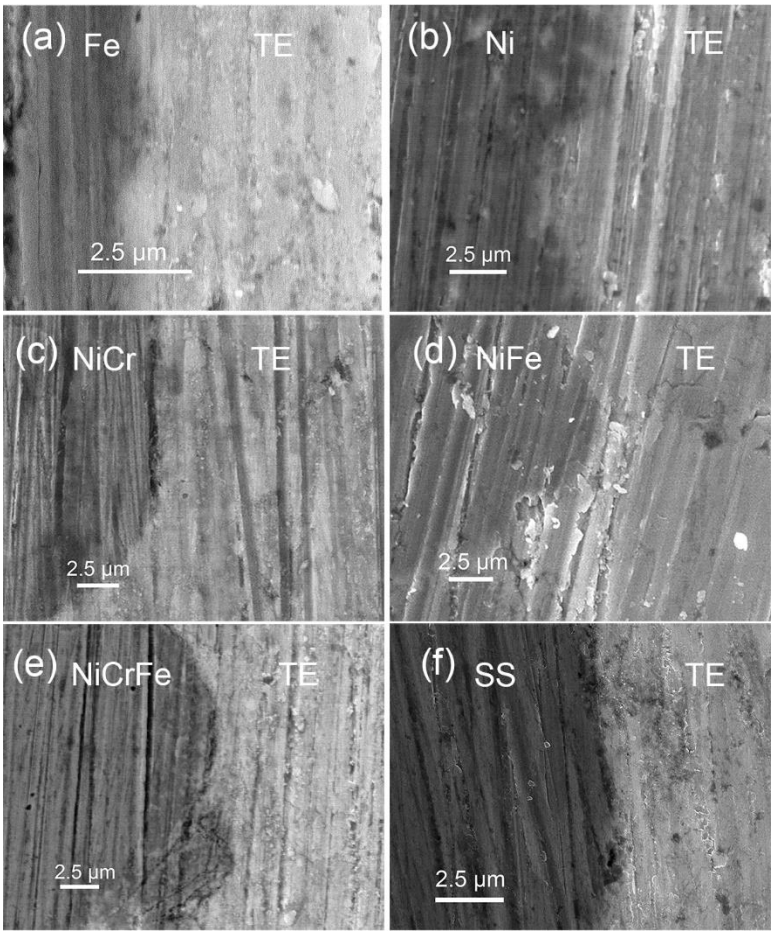

Figure S5. Microstructural morphology of the as-prepared contact interfaces in the single M/TE leg composed of $Mg_{3+\delta}Bi_{1.5}Sb_{1.5}$ and (a) Fe, (b) Ni, (c) NiCr, (d) NiFe, (e) NiCrFe, and (f) stainless steel (SS).

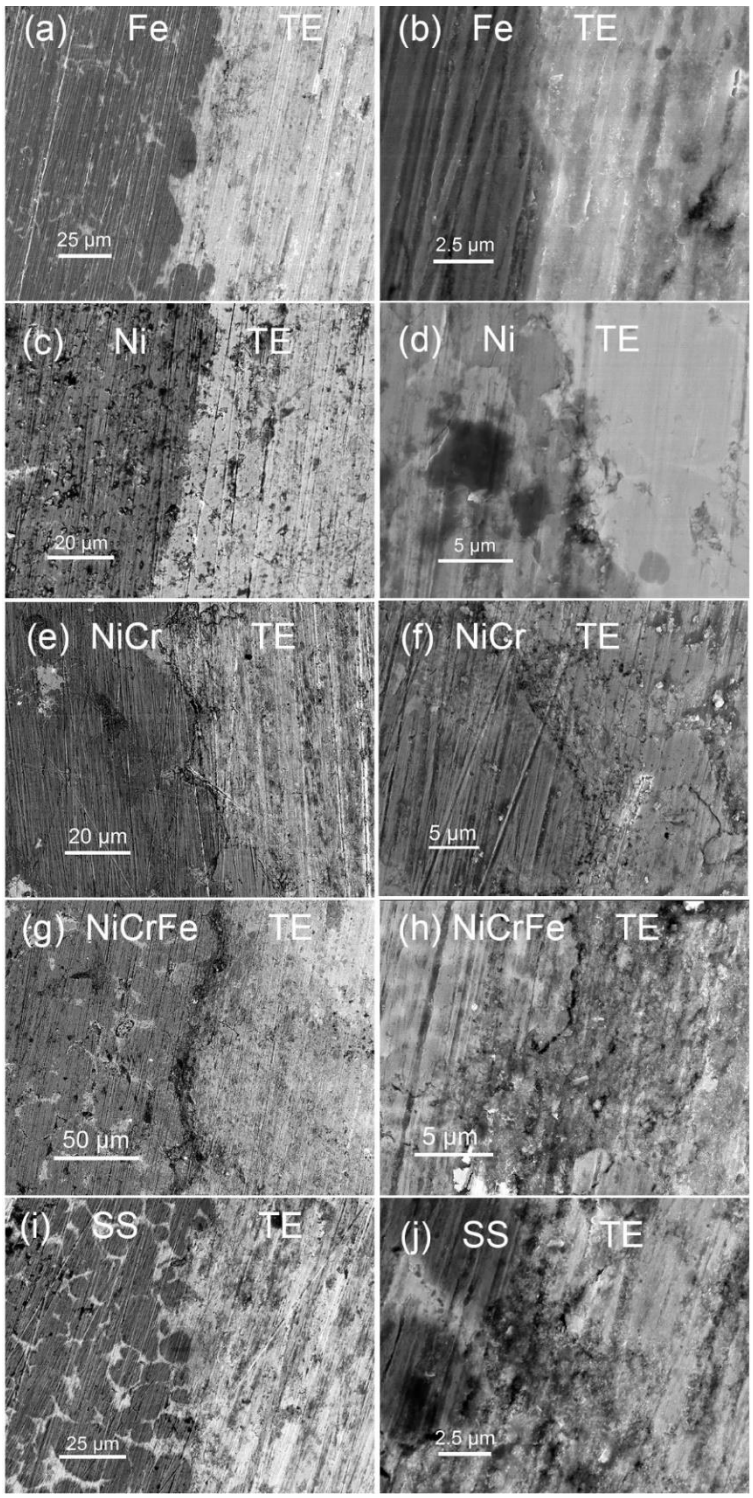

Figure S6. Microstructural morphology of the contact interfaces in the single M/TE leg composed of $Mg_{3+\delta}Bi_{1.5}Sb_{1.5}$ and (a,b) Fe, (c,d) Ni, (e,f) NiCr, (g,h) NiCrFe, and (i,j) stainless steel (SS) after aging and thermal cycling and quenching test.

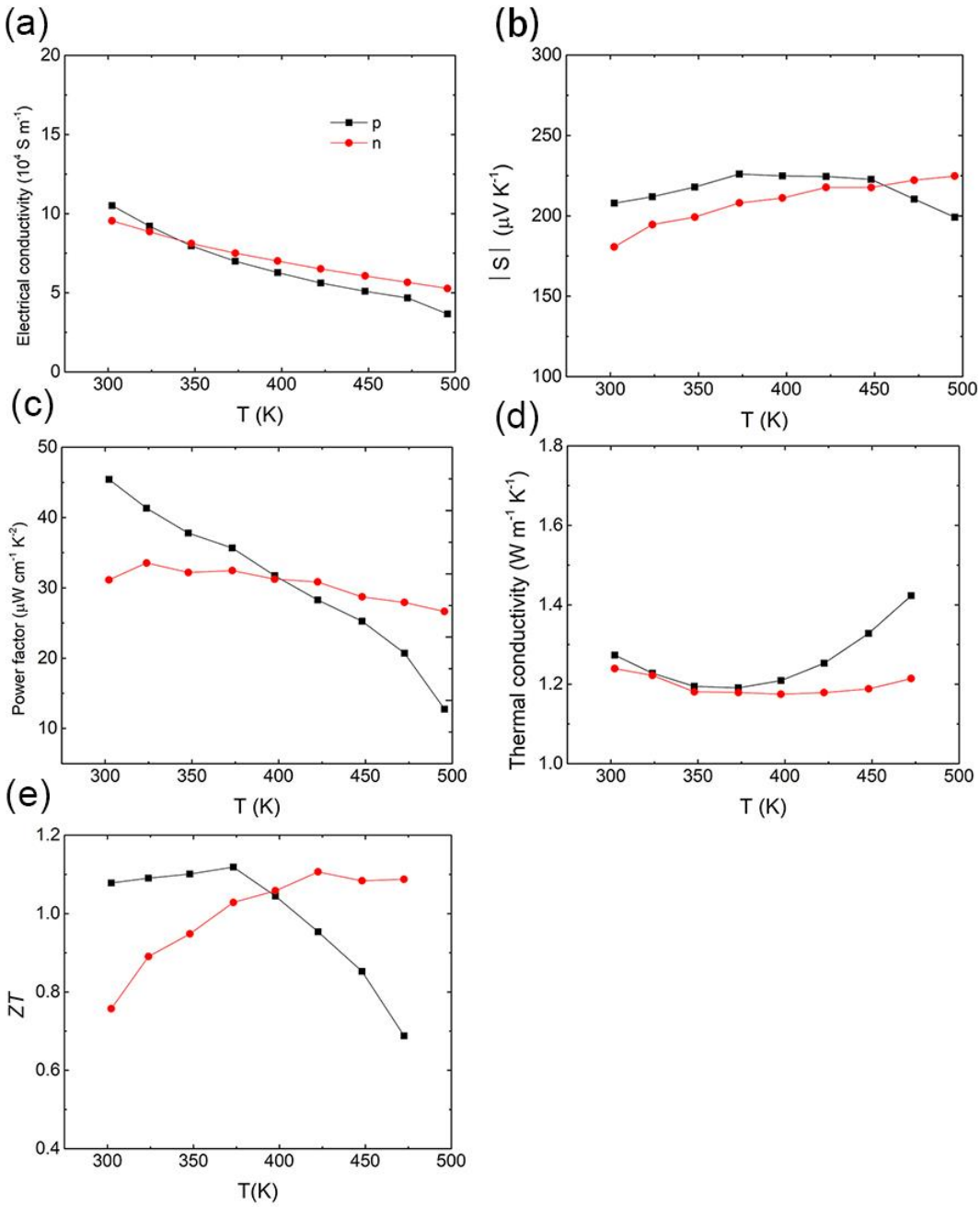

Figure S7. Thermoelectric properties of n-type $Mg_{3+\delta}Bi_{1.5}Sb_{0.5}$ and p-type $Bi_{0.4}Sb_{1.6}Te_3$.

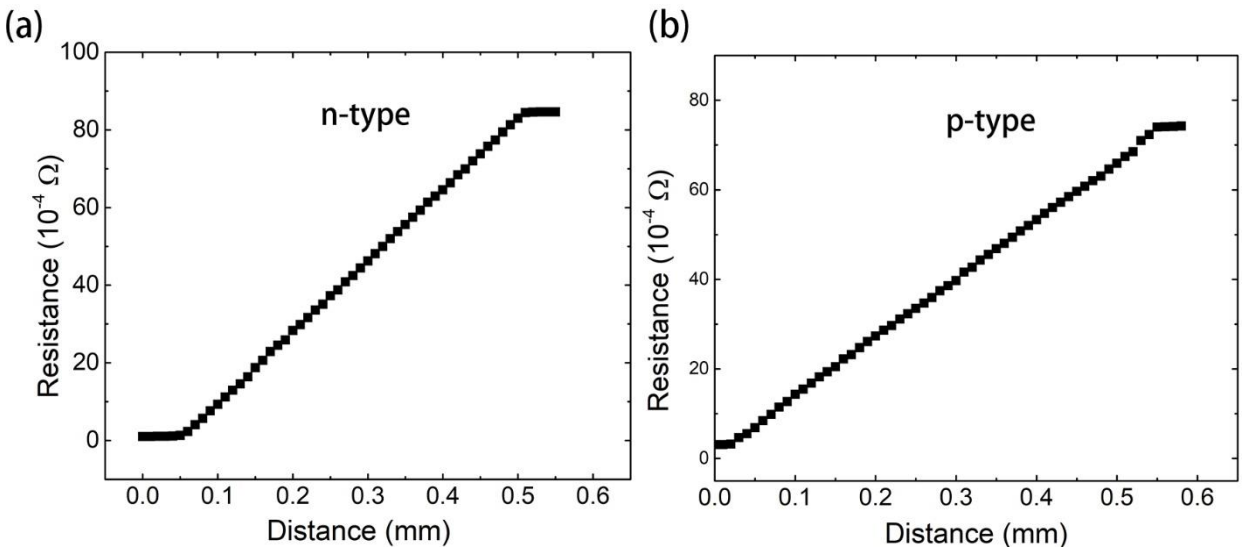

Figure S8. The measured contact resistance of (a) NiFe/$Mg_{3+\delta}Bi_{1.5}Sb_{0.5}$/NiFe and (b) Fe/$Bi_{0.4}Sb_{1.6}Te_3$/Fe. The n-type NiFe/$Mg_{3+\delta}Bi_{1.5}Sb_{0.5}$/NiFe exhibits the contact resistance of $7.6 \times 10^{-6}\ \Omega\ cm^{-2}$ and p-type Fe/$Bi_{0.4}Sb_{1.6}Te_3$/Fe has the contact resistance of $1.25 \times 10^{-5}\ \Omega\ cm^{-2}$.